31 August 2001

ELSEVIER

Chemical Physics Letters 344 (2001) 434–440

CHEMICAL PHYSICS LETTERS

www.elsevier.com/locate/cplett

The effect of substrate topography on the local electronic structure of WS_2 nanotubes

O. Tal [a], M. Remskar [b], R. Tenne [c], G. Haase [a,*]

[a] *Department of Chemical Physics, The Weizmann Institute of Science, Rehovot 76100, Israel*
[b] *Department of Solid-State Physics, Jozef Stefan Institute, Jamova 39, SI-1000 Ljubljana, Slovenia*
[c] *Department of Materials and Interfaces, The Weizmann Institute of Science, Rehovot 76100, Israel*

Received 23 February 2001; in final form 2 July 2001

Abstract

We explore the possibility of controlling electronic properties along an inorganic nanotube (INT) through the influence of nanometer-scale features in the underlying substrate. We examined single multi-walled WS_2 INTs using scanning tunneling microscopy (STM) in high vacuum. As long as the INTs lie flat on MoS_2 (0 0 0 1) or graphite (0 0 0 1) surfaces, they appear semimetallic. However, when the INT is suspended above the surface due to crossing steps or other nanotubes, a band gap opens up. We discuss this observation in terms of either a potential drop under the INT, or a change in its electronic properties due to its distortion when it lies flat on a surface.

1. Introduction

The ultimate device miniaturization would be to use individual molecules as functional electronic devices. Single-wall carbon nanotubes (CNTs) were offered as promising candidates for achieving this goal [1]: depending on their diameter and chirality, they are either one-dimensional metals or semiconductors [2]. Inter- or intramolecular junctions in single-walled CNTs (say, consisting of a pentagonal and a heptagonal defect) are potentially ideal structures for building robust, molecular-scale electronics. The latter junctions have been studied theoretically [3,4], as well as experimentally, where scanning probe microscopy was used to determine their atomic structure and electronic properties [5–9]. Nevertheless, although different CNT-based structures were already demonstrated to have various electronic behaviors, ranging from a rectifying diode [5] to a double quantum dot [6], it is still very difficult to control the growth of nanotube structures. Also, CNT-based devices may not be stable in air, as their electronic properties change upon oxidation [10,11] or interaction with water vapor [12].

Inorganic nanotubes (INTs) made of transition metal dichalcogenides [13] have been scarcely studied: MoS_2 and WS_2 INTs were shown to be always semiconducting and very inert chemically [14]. Although some multi-walled WS_2 or MoS_2 INTs have many defects in their outer shells, the inner nested tubes seem to be continuous and intact [15–17].

In this Letter, we wish to explore the possibility of tailoring the local electronic properties of segments along the latter INTs, through the influence

* Corresponding author. Fax: +972-8-9344123.
E-mail address: gad.haase@weizmann.ac.il (G. Haase).

0009-2614/01/$ - see front matter
PII: S0009-2614(01)00813-2

of nanometer-sized features in the underlying substrate. We make use of scanning tunneling microscopy (STM) and spectroscopy (STS) to distinguish between 'metallic' and 'semiconducting' regions in the nanotubes.

2. Experiment

WS_2 nanotubes were grown by chemical transport, using iodine as a transporting agent [17]. The main problem that we faced, when attempting to image these INTs with STM at room temperature, was the fact that the metal dichalcogenide INTs could hardly ever be found on Au(1 1 1), highly ordered pyrolytic graphite (HOPG) or MoS_2 (0 0 0 1) flat surfaces. The reason is probably embedded in the fact that these inorganic fullerenes are very inert and were shown to be very good lubricants [18]. As a result, they slide freely at the surface. The data presented here was taken on a few nanotubes that we managed to image on MoS_2 crystal terraces, as well as on nanotubes that were captured on, or near etch-pits on HOPG surfaces. Even when the INTs seemed fixed in their position, we could not obtain atomically-resolved images of their structure (probably due to large thermal motion).

The MoS_2 and HOPG substrates were prepared by pealing the upper layers with an adhesive tape. An intermediate grade HOPG substrate was heated in air to 650 °C to form flat-bottomed circular etch-pits, a few carbon layers deep [19].

A WS_2 INT suspension was prepared as follows: 1 mg INT powder was added to 2–4 ml of absolute ethanol (AR, Bio-Lab) and sonicated in a low power ultrasonic bath (Mettler Electronics) for 10 min to decompose large grains, followed by a sonication with a high power ultrasonic finger (Sonics & Materials, model: CV 26) for 20 min at 40% power. Transmission electron microscopy (TEM) imaging before and after sonication showed that the nanotubes were not fragmented, but that excess amorphous material was removed from them. A drop of the freshly prepared nanotube suspension was deposited directly on the substrates and the solvent was allowed to dry in vacuum.

The STM and STS measurements were performed with an Omicron (UHV-1) STM head in high vacuum (10^{-9}–10^{-7} Torr) to avoid tunneling current-induced reactions with ambient air. The STM head was driven by a Topometrics electronics unit. The original Omicron in-vacuum I–V converter was replaced by a $\times 10$ faster circuit to improve spectroscopy speed and accuracy.

3. Results

Fig. 1a shows TEM (Philips CM120) images of a typical WS_2 nanotube: most of the INTs had complete layers but no caps at their ends. Some of the nanotubes, however, had their outer layers broken, giving rise to a high density of steps (see Fig. 1b). The diameter of the tubes ranged from 10 to 100 nm and was not always fixed along the INTs' axis, although the number of the inner walls did not seem to vary. TEM–energy dispersive X-ray spectroscopy (EDS) analysis revealed that some of the iodine was still present in the nanotubes. Iodine residue is likely to produce an n-doping effect.

Fig. 2 shows a typical set of I–V curves that were averaged on top WS_2 INTs that were lying flat on flat terraces, both at MoS_2 (0 0 0 1) (a) and at HOPG (b) surfaces (dashed lines), as well as I–V curves that were taken on the corresponding clean substrates (solid lines). Although the I–V curves on the clean MoS_2 (0 0 0 1) surface exhibit a band

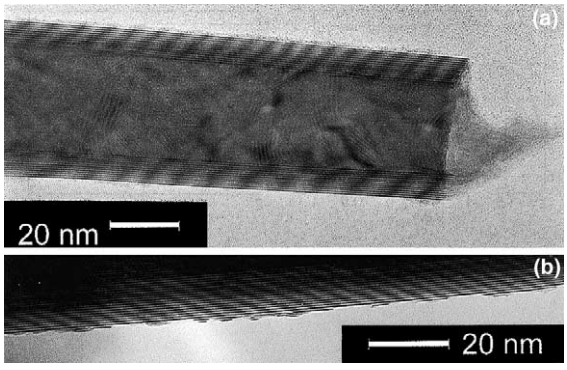

Fig. 1. TEM images (120 kV) of a typical WS_2 nanotubes (a) and a closer view at the surface of a nanotube with broken outer shells (steps) (b).

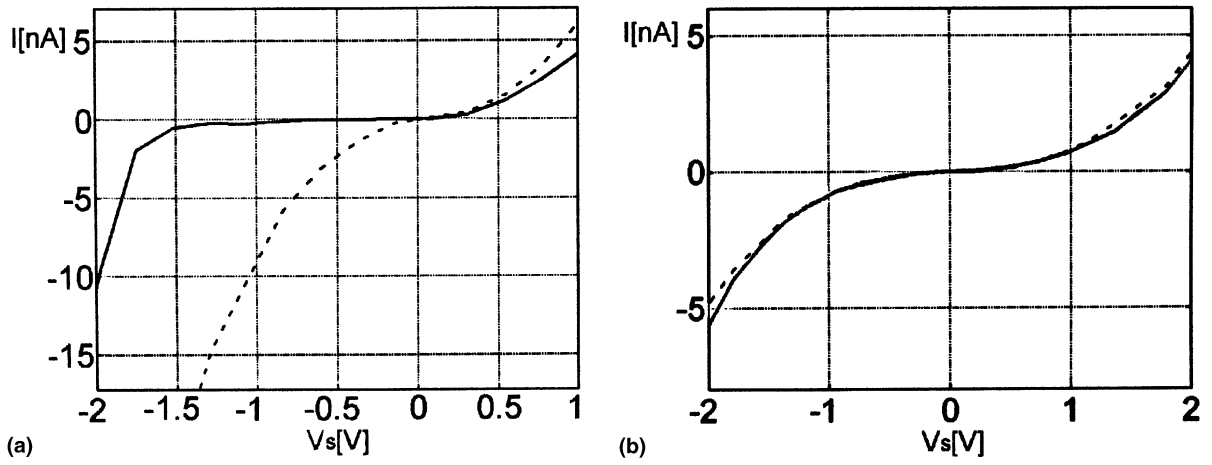

Fig. 2. *I–V* curves on top WS_2 nanotubes (dashed line) and on the clean substrate (solid line), on MoS_2 (0 0 0 1): (a) height stabilized at $V_s = +0.5$ V, $I_t = 1$ nA) and on HOPG (b) $V_s = +0.68$ V, $I_t = 0.4$ nA) surfaces.

gap, the *I–V* curves on top of the INTs, adsorbed on both surfaces, show a weak metallic behavior, similarly to *I–V* curves that were taken on the clean HOPG. As long as straight INTs were adsorbed in intimate contact with flat terraces, all *I–V* curves taken on top of them appeared identical.

It is important to note that on HOPG, for example, the deposited INTs may be easily confused with graphene sheets that are rolled upon themselves at steps [20,21], or subsurface graphene ribbons [21]. In order to avoid such misinterpretations, we chose to ignore all features that reside between two terraces of different heights. In addition, we ignored nanotube structures that did not have a bend, a fork-like split, or appeared as a twisted rope, to avoid subsurface ribbons.

A single WS_2 nanotube (or maybe a bundle), which is lying over a rope of WS_2 nanotubes and over a multilayered trench in the HOPG substrate, is shown in Fig. 3. Careful analysis of various features in the image led us to believe that the appearance of the nanotube as a bundle of parallel tubes is due to convolution with the tip apex shape (a multiple tip effect). Unfortunately, when dealing with features that protrude more than a few nm above the surface, this is almost unavoidable. It is assumed here that the location of the topographically highest INT in the apparent bundle is imaged in the correct location in respect to the other

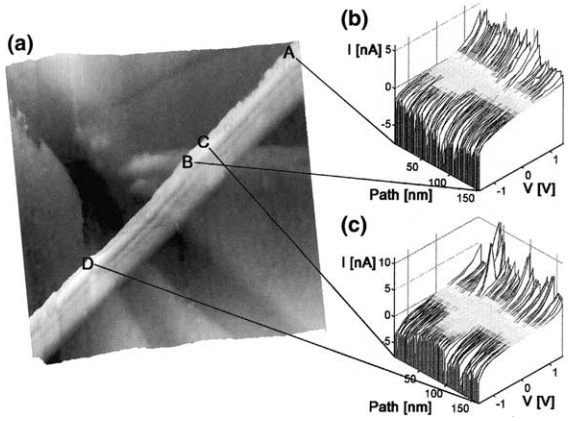

Fig. 3. (a) A STM constant current topography image (340 nm × 340 nm) of a WS_2 INT on an HOPG surface with trenches and an underlying INT rope ($V_s = +0.73$ V and $I_t = 0.4$ nA), (b) a sequence of *I–V* curves along a path between points A and B, and (c) between C and D.

surface features. The diameter of this nanotube and the depth of the trench are 15 ± 5 and 3 nm, respectively.

Consider the path between points A and B on the nanotube in Fig. 3a. A series of *I–V* curves along this path is presented in Fig. 3b, where the tip height was stabilized before each *I–V* spectroscopy measurement to give 0.4 nA at $V_s = +0.73$ V. Up to a certain point on this path, the *I–V* curves exhibit a weakly metallic character,

as was seen in the case of the INTs that were lying flat, in contact with the HOPG surface (Fig. 2b). At about 80 nm before the nanotube crosses the underlying rope, a zero current plateau appears in Fig. 3b, that corresponds to an opening of a band gap of 0.6 ± 0.1 eV with a non-degenerate n-type nature. The band gap is closed slightly before the point in which the INT approaches the nanotube rope.

A series of *I–V* curves along the path between C and D is shown in Fig. 3c. As in Fig. 3b. the *I–V* curves exhibit a metallic-like shape except at a well defined segment that is suspended between the rope crossing and the trench edge. In this region, once more, a band gap is opened (0.8 ± 0.1 eV) and it is shifted to the negative sample-bias voltage direction.

Fig. 4a shows a WS_2 INT that lies over a multilayered-deep etched pit in the HOPG substrate. The nanotube diameter and the pit depth are estimated as 25 ± 5 and 4 nm, respectively. A sequence of *I–V* curves that were taken along a path, which is marked by a solid black line on the nanotube in Fig. 4a, can be seen in Fig. 4b. Again, along most of the path, the *I–V* curves exhibit a weak metallic character. However, at the region that is located inside the pit, right before the pit edge, a pronounced band gap is opened along a path of 5.4 nm. The apparent band gap, if determined by the bias values where the current deviates by 0.1 nA from zero, averaging on many curves, is 1.0 ± 0.1 eV. Once more, the nanotube segment that is suspended above the surface has a non-degenerate n-type semiconductor nature.

When examining nanotubes with respect to specific underlying features in the substrate surface, one should be aware of the possibility that due to the large diameter of the INTs, multi-apex tips would give rise to wrong images, where shallow surface features appear in close proximity to INTs that are actually situated far away from them. Nevertheless, both for Figs. 3a and 4a, a superposition of each of these features and an INT that is lying elsewhere will produce an *I–V* curve that contains a sum of their contributions. As seen in Fig. 2, INTs that lie flat on HOPG surfaces have an *I–V* curve with a nearly metallic shape. A trench and a pit in HOPG surfaces also give rise to a weakly metallic-shaped *I–V* curves, whereas, *I–V* curves that were taken on the edge of a trench or a pit sometimes appear even more metallic. Therefore, a superposition of an INT and a surface feature due to a tip with two widely spaced apexes is expected to produce a metallic shaped *I–V* curve as well.

Finally, Fig. 5a presents a single zig-zag shaped WS_2 INT on a MoS_2 (0 0 0 1) surface. A larger view of this nanotube reveals that it has numerous bends that are not all in the same plane. Note that once more, this INT is accompanied by 'ghost' images of itself that are caused by a multiple-tip effect. The apparent band gap that is depicted in the *I–V* curves in Fig. 5b was extracted from data that were taken at the top of the (brighter) INT along the marked black solid line in Fig. 5a. The *I–V* curves indicate that an apparent gap of 0.7 ± 0.2 eV exists along most of the nanotube. However, at the bends, and at a few other random

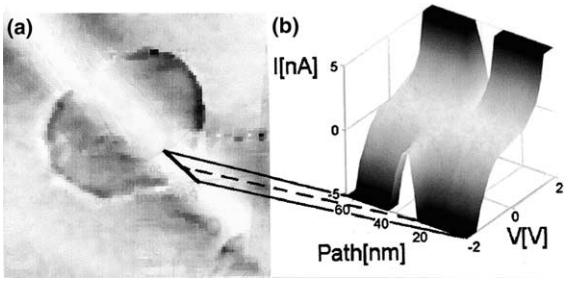

Fig. 4. (a) A STM constant current topography image (380 nm × 380 nm) of a WS_2 nanotube adsorbed over an etched pit on HOPG ($V_s = +0.75$ V and $I_t = 0.4$ nA). (b) A sequence of *I–V* curves along the dark line.

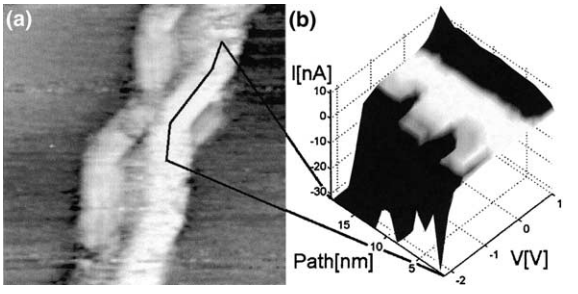

Fig. 5. (a) A single, WS_2 nanotube with bends on an MoS_2 (0 0 0 1) surface, (44 nm × 44 nm, $V_s = +0.5$ V and $I_t = 1$ nA), and (b) a sequence of *I–V* curves along a path that is outlined on the nanotube.

locations, the I–V curves exhibit a metallic-like behavior.

4. Discussion

The difference in electronic behavior, between a WS_2 INT lying flat on a terrace and an INT suspended above it, may stem from inherent properties of the investigated system, or from its relation with the STM apparatus. The latter option will be discussed first.

The potential difference between the tip and the topmost surface of an adsorbed nanotube would depend on how much of the sample bias voltage (V_s) drops across the nanotube itself. An additional voltage drop can occur across a gap that may exist between the substrate and the nanotube, and within the substrate itself, if it is semiconducting (see for example [22–24]. It is possible that the latter effect is the only explanation for the appearance of a widened energy gap ('weak-metallic to semiconducting' transition) that we observed for INT segments that are suspended above the surface. In order to estimate the above effect, we solved numerically the Poisson equation in three dimensions. Since the INTs diameter is of the order of an exciton diameter [25], and since we do not know anything about the nature of the barrier and the band alignment between the substrate and the INT, we represent the WS_2 nanotube as a dielectric matter (no free carriers, with a dielectric constant of $\varepsilon = 7$ [25]). The STM tip is introduced as a flat equi-potential surface, located 2 nm above the INT. Placing a 15 nm diameter nanotube over a 50 nm wide and 3 nm deep trench in a metallic surface, which is biased at V_s in respect to the tip, makes a band gap of 0.2 eV appear as $\sim$0.9 eV above the trench and $\sim$0.6 eV away from it. Adding the electron and hole densities, which are dependent on the tip-induced band bending, would limit the resulting apparent band gap.

The above model assumes that a WS_2 INT, which lies flat on the substrate surface, is unperturbed, and that it exhibits a weak metallic nature or a small band gap of $\sim$0.1 eV. However, full electronic calculations by Seifert et al. for single-walled MoS_2 [26] and WS_2 [27] INTs showed that the bulk $\sim$1.3 eV band gap shrinks with decreasing tube diameters, yet does not vanish in the diameter range of the INTs we used. The weakly metallic appearance could also stem from surface states due to the abundance of steps: a few of the INTs that were imaged with TEM (see Fig. 1b) indeed showed fragmented outer layers. In this case, the density of surface states per unit area due to such steps is most likely not sufficient to prohibit tip-induced band bending [28]. Therefore, although the electrostatic effect on the apparent band gap should be always taken into consideration for non-metallic INTs, it cannot account solely for such a pronounced difference between suspended and non-suspended INT segments. We, hence, proceed to the next possible explanation.

Metal-induced gap states (MIGS) at metal–semiconductor junctions [29,30], that stem from the decay of the metal electron wave functions into a semiconductor, may reach the vacuum side of an adsorbed semiconducting INT and give rise to the measured weakly metallic I–V curves. This would also explain the absence of the weakly metallic behavior when a segment of the INT is suspended above the surface. The existence of MIGS was also offered as a possible explanation for the observation of finite currents around zero voltage, in STS that was taken on semiconducting single-walled CNTs on a gold substrate [3]. However, while the diameter of a single-walled CNT is about 1–2 nm, our INTs' diameter is over one-order of magnitude larger. Also, the same metallic behavior was observed when the nanotubes were lying flat on a semiconducting non-degenerate (MoS_2) substrate.

The last model that is consistent with our observation is based on the fact that an INT that lies on a flat surface undergoes a geometrical deformation. It turns out that van der Waals forces are sufficient to make CNTs' cross-sections no longer circular, as was previously shown both experimentally and by calculations [31,32]. It was recently suggested that such a deformation will make a semiconducting CNT metallic [33]. In the case of multi-walled WS_2 nanotubes the deformation will be smaller due to the large number of layers, as well as due to the relatively higher stiffness of each individual layer (consisting of S–W–S planes). The strain energy of a single-walled WS_2 nanotube was

calculated to be one-order of magnitude larger than that of a single-walled CNT with a similar diameter [34]. Based on the elastic properties of a single layer, one can estimate the distortion of a multi-walled WS_2 nanotube (six layers, 15 nm in diameter) to be 0.5 nm (3.3%) in the direction perpendicular to the surface [35]. In fact, the radius of curvature of the INT layers, along the lines where they depart from the surface, becomes even smaller.

The calculations by Seifert et al. [26,27] showed a decrease in the band gap of single-walled (n,n) and $(n,0)$ MoS_2 and WS_2 nanotubes as their diameter decreased. For WS_2, only for zig-zag $(n,0)$ nanotubes the band gap tends to vanish for diameters <10 Å. The above mentioned reduction in the radius of curvature of the nanotube next to the surface would similarly shift the electronic bands and reduce the energy gap. If this is indeed the case, we expect the original (undistorted) INT band gap to exist in segments that hover above the surface and do not have contact with underlying nanotube structures.

The curved INT in Fig. 5 offers us the opportunity to look at the effect of bends in an INT that probably does not lie flat on the substrate surface (MoS_2 (0 0 0 1)). The latter bends change the INT radius of curvature locally through local changes in the unit cell structure (say, squares instead of hexagons), rather than due to a distortion by the van der Waals forces that attract it to the surface, or by crossing other nanotube ropes. Nevertheless, the I–V curves at the bends also exhibit a weak metallic character (or a closure of the band gap) either through the strain effect on the layers or due to the introduction of new gap states by the irregular unit cells.

5. Conclusions

We have shown that WS_2 nanotubes that lie on a flat surface, be it of a semiconductor (MoS_2) or a semimetal (HOPG) substrate, exhibit a weak metallic behavior. However, I–V curves that were taken on top single WS_2 INTs that were suspended above the surface, show a semiconductor character. It is plausible that the observed energy gap variations stem mainly from the fact that part of the voltage between the tip and the back of the sample drops on the vacuum gap between the nanotube and the underlying surface. Nevertheless, we also argue that the INTs appear metallic when they lie flat on the substrate surface because of a distortion of their cross-section due to the van der Waals forces that pull them together. When the INT is suspended above the surface, the distortion is lifted and the energy gap reappears. Finally, WS_2 INTs, which are naturally bent in a few places, show an enhanced metallic behavior at the bends locations, suggesting once more that a local distortion (though not due to stress) can bring about the filling of the energy gap.

The results of this work open new avenues for obtaining control over the electronic properties of nanotubes by patterning the substrates on which they would be deposited. This may allow the integration of metal–semiconductor junctions in a room temperature, chemically-stable nanotube-based electronic device.

Acknowledgements

This research was supported by the Israeli Science Foundation administered by the Israel Academy of Sciences and Humanities. We are grateful to Dr. Ronit Popovitz-Biro for her TEM expertise, as well as to Prof. Israel Rubinstein and Dr. Alexander Vaskevitch for advice regarding sample preparation.

References

[1] P.G. Collins, A. Zettl, H. Bando, A. Thess, R.E. Smalley, Science 278 (1997) 100.
[2] J.W.G. Wildoer, L.C. Venema, A.G. Rinzler, R.E. Smalley, C. Dekker, Nature 391 (1998) 59.
[3] L. Chico, V.H. Crespi, L.X. Benedict, S.G. Louie, M.L. Cohen, Phys. Rev. Lett. 76 (1996) 971.
[4] R. Tamura, M. Tsukada, Phys. Rev. B 61 (2000) 8548.
[5] Z. Yao, H. Postma, L. Balents, C. Dekker, Nature 402 (1999) 273.
[6] J. Lefebvre, R.D. Antonov, M. Radosavljevic, J.F. Lynch, M. Llaguno, A.T. Johnson, Carbon 38 (2000) 1745.
[7] M. Ouyang, J.-L. Huang, C.L. Cheung, C.M. Lieber, Science 291 (2001) 97.

[8] H.W.C. Postma, M. de Jonge, Z. Yao, C. Dekker, Phys. Rev. B 62 (2000) R10653.
[9] M.S. Fuhrer, J. Nygard, L. Shih, M. Forero, Y. Young-Gui, M.S.C. Mazzoni, C. Hyoung Joon, I. Jisoon, S.G. Louie, A. Zettl, P.L. McEuen, Science 288 (2000) 494.
[10] P.G. Collins, K. Bradley, M. Ishigami, A. Zett, Science 287 (2000) 1801.
[11] J. Seung-Hoon, S.G. Louie, M.L. Cohen, Phys. Rev. Lett. 85 (2000) 1710.
[12] A. Zahab, L. Spina, P. Poncharal, C. Marliere, Phys. Rev. B 62 (2000) 10000.
[13] R. Tenne, L. Margulis, M. Genut, G. Hodes, Nature 360 (1992) 444.
[14] G.L. Frey, S. Elani, M. Homyonfer, Y. Feldman, R. Tenne, Phys. Rev. B 57 (1998) 6666.
[15] Y.Q. Zhu, W.K. Hsu, H. Terrones, N. Grobert, B.H. Chang, M. Terrones, B.Q. Wei, H.W. Kroto, D.R.M. Walton, C.B. Boothroyd, I. Kinloch, G.Z. Chen, A.H. Windle, D.J. Fray, J. Mater. Chem. 10 (2000) 2570.
[16] A. Rothschild, R. Popovitz-Biro, O. Lourie, R. Tenne, J. Phys. Chem. B 104 (2000) 8976.
[17] M. Remskar, Z. Skraba, M. Regula, C. Ballif, R. Sanjines, F. Levy, Adv. Mater. 10 (1998) 246.
[18] L. Rapoport, Yu. Bilik, Y. Feldman, M. Homyonfer, S.R. Cohen, R. Tenne, Nature 387 (1997) 791.
[19] D.L. Patrick, V.J. Cee, T.P. Beebe, Science 265 (1994) 231.
[20] H.V. Roy, C. Kallinger, K. Sattler, Surf. Sci. 407 (1998) 1.
[21] F. Atamny, T.F. Fassler, A. Baiker, R. Schlogl, Appl. Phys. A 71 (2000) 441.
[22] R.M. Feenstra, J.A. Stroscio, J. Vac. Sci. Technol. B 5 (1987) 923.
[23] M. Weimer, J. Kramar, J.D. Baldeschwieler, Phys. Rev. B 39 (1989) 5572.
[24] G. Haase, Int. Rev. Phys. Chem. 19 (2000) 247.
[25] G.L. Frey, R. Tenne, M.J. Matthews, M.S. Dresselhaus, G. Dresselhaus, J. Mater. Res. 13 (1998) 2412.
[26] G. Seifert, H. Terrones, M. Terrones, G. Jungnickel, T. Frauenheim, Phys. Rev. Lett. 85 (2000) 146.
[27] G. Seifert, H. Terrones, M. Terrones, G. Jungnickel, T. Frauenheim, Solid State Commun. 114 (2000) 245.
[28] J.R. Lince, D.J. Carre, P.D. Fleischauer, Phys. Rev. B 36 (1987) 1647.
[29] W. Moench, Prog. High Temp. Supercond. 18 (1989) 298.
[30] E.H. Rhoderick, R.H. Williams, Metal–Semiconductor Contacts, Oxford, Claredon, 1988.
[31] R.S. Ruoff, J. Tersoff, D.C. Lorents, S. Subramoney, B. Chan, Nature 364 (1993) 514.
[32] T. Hertel, R.E. Walkup, P. Avouris, Phys. Rev. B 58 (1998) 13870.
[33] C. Kilic, S. Ciraci, O. Gulseren, T. Yildirim, Phys. Rev. B 62 (2000) R16345.
[34] U.S. Schwarz, S. Komura, S.A. Safran, Europhys. Lett. 50 (2000) 762.
[35] U.S. Schwarz, S.A. Safran, 2000, Private communication.